

Cite this: *RSC Adv.*, 2015, 5, 6985

# Cathepsin B-sensitive cholesteryl hemisuccinate–gemcitabine prodrug nanoparticles: enhanced cellular uptake and intracellular drug controlled release

Yanyun Xu,<sup>a</sup> Jianqi Geng,<sup>b</sup> Ping An,<sup>a</sup> Yan Xu,<sup>a</sup> Jin Huang,<sup>ab</sup> Wei Lu,<sup>a</sup> Shiyuan Liu<sup>c</sup> and Jiahui Yu<sup>\*a</sup>

Gemcitabine [2',2'-difluoro-2'-deoxycytidine (dFdC)], firstline treatment for pancreatic cancer in the clinic, is a cytotoxic nucleoside analogue. Nucleoside transporters are required in the transport of gemcitabine into cells since it is a hydrophilic compound. Actually, there are significant drawbacks for the application of gemcitabine in clinic, including a short half-life and serious side effects. In order to overcome the mentioned drawbacks, a novel prodrug, cholesteryl hemisuccinate–gemcitabine (CHSdFdC), was synthesized through covalently coupling the amino group of gemcitabine with the carboxylic group of cholesteryl hemisuccinate. The amphiphilic prodrug self-assembled spontaneously as nanoparticles in aqueous media confirmed by transmission electron microscopy (TEM). Dynamic light scattering (DLS) measurement revealed that the mean particle size is approximately 200 nm in aqueous media. The CHSdFdC nanoparticles displayed accumulative controlled drug release in simulated lysosome conditions (pH 5.0 NaAc buffer solution containing cathepsin B); the amount of drug release reached up to 80% within 10 h. However, there was almost no drug release in pH 7.4 PBS and pH 5.0 NaAc buffer solutions without cathepsin B. All these results indicated the intracellularly controlled drug release manner of the CHSdFdC nanoparticles. The controlled release of dFdC from the CHSdFdC nanoparticles was related closely to cleavage of amide bonds by cathepsin B. The CHSdFdC nanoparticles exhibited increased ability to inhibit cell growth compared with gemcitabine *in vitro*. Meanwhile, the CHSdFdC nanoparticles exhibited enhanced cellular uptake ability against Bxpc-3 cells, and the amount of CHSdFdC was about 15 fold of gemcitabine during the 2.5 h incubation. All these results showed that the CHSdFdC nanoparticle prodrug has great potential in the treatment of pancreatic cancer.

Received 12th November 2014  
Accepted 15th December 2014

DOI: 10.1039/c4ra13870h

www.rsc.org/advances

## 1 Introduction

Gemcitabine [2',2'-difluoro-2'-deoxycytidine (dFdC)] has been proved to be a potent cytotoxic nucleoside analogue which demonstrated efficacy in the treatment of various solid tumors, including colon, lung, pancreatic, breast, bladder and ovarian cancers.<sup>1–3</sup> In order to achieve therapeutic effects, gemcitabine must be transported into cells. Membrane proteins called nucleoside transporters are required in the transport of gemcitabine because it is a hydrophilic compound. The main transporter types include hENT<sub>1</sub>, hENT<sub>2</sub>, hCNT<sub>1</sub> and hCNT<sub>3</sub>.<sup>4</sup>

Nucleoside transporter deficiency would make it difficult for gemcitabine to be transported into cells. In addition, as a traditional chemotherapeutic drug, gemcitabine is difficult to accumulate at tumor tissue selectively, which lead to undesired side effects and inadequate drug concentrations reaching tumor, despite it is a primary drug for cancer treatment.<sup>5–8</sup> In this paper, in order to make it easier for gemcitabine to enter cells, especially nucleoside transporter deficiency cells, the cholesteryl-hemisuccinate–gemcitabine conjugate was fabricated into nanoparticles to change the approach that gemcitabine enter cells. As a result, gemcitabine would enter cells *via* endocytosis rather than transport by nucleoside transporters. In addition, nanodrug delivery system could use enhanced permeability and retention (EPR) (Fig. 1) effect to promote the drugs targeting tumor tissue selectively, leading to potentially enhanced antitumor effect and decreased side effects.<sup>9–14</sup> Numerous nanodrug or nanaodrug candidates have been approved for clinical applications or under clinical trials at different stages.<sup>13,15,16</sup> After being transported into cells, a part of

<sup>a</sup>Institute of Drug Discovery and Development, Shanghai Engineering Research Center of Molecular Therapeutics and New Drug Development, East China Normal University, Shanghai 200062, PR China. E-mail: jhyu@sist.ecnu.edu.cn; Fax: +86 21 6223 7026; Tel: +86 21 6223 7026

<sup>b</sup>College of Chemical Engineering, Wuhan University of Technology, Wuhan 430070, PR China

<sup>c</sup>Department of Diagnostic Imaging, ChangZheng Hospital, Shanghai, 200003, PR China



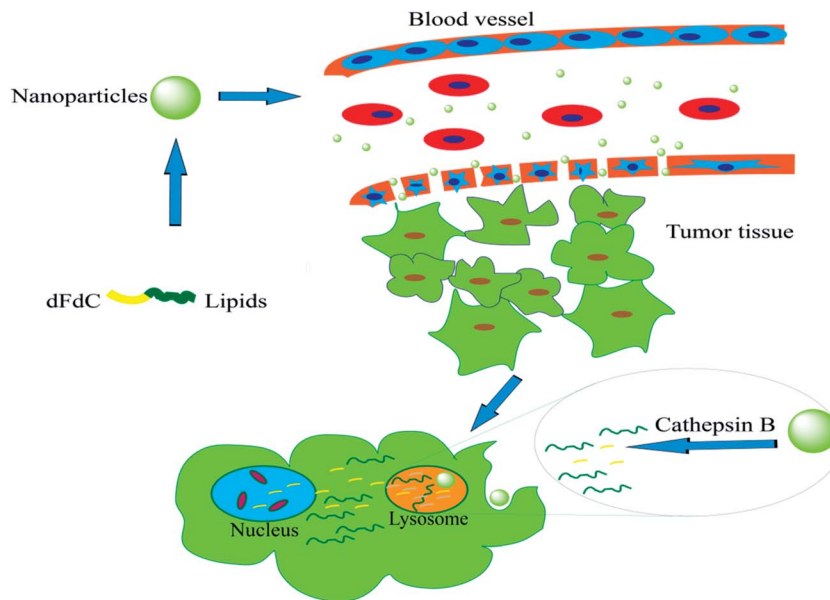


Fig. 1 Illustration of EPR effect and intracellularly controlled release of dFdC from CHSdFdC.

gemcitabine is deaminized by cytidine deaminase into inactive uracil derivative (dFdU) intracellularly, hence resulting in a short half-life.<sup>17</sup> Acylation of N<sup>4</sup>-amino group of the pyrimidine ring of dFdC would protect the amino group from being rapidly degraded by cytidine deaminase. Taking the strategy of nano-drug delivery system, Couvreur's group covalently coupled gemcitabine with squalenic acid, and the resultant 4-(N)-tris-nor-squalenoyl-gemcitabine (SQdFdC) prodrug self-assembled into nanoparticles, which were shown to overcome gemcitabine resistance in murine leukemia cells (*i.e.*, L1210 10K),<sup>18</sup> human leukemia cells (*i.e.*, CEM/ARAC8C),<sup>18</sup> and human pancreatic cancer cells (*i.e.*, Panc-1).<sup>19</sup> It was concluded that SQdFdC nanoparticles enabled the partial circumvention of three well-known resistance mechanisms to gemcitabine, including the deficiency of nucleoside transporters, insufficient activity of deoxycytidine kinase (dCK), and inactivation by deaminases.<sup>20</sup> Zhengrong Cui *et al.* have reported that 4-(N)-stearoyl gemcitabine (GemC18), a stearic acid amide derivative of gemcitabine, could effectively inhibit the growth of gemcitabine resistance TC-1-GR tumors in mice, and in contrast, the molar equivalent dose of gemcitabine hydrochloride did not show any activity against the growth of the TC-1-GR tumors.<sup>21</sup>

Cholesterol is an indispensable substance in the formation of cell membranes. As the basic component of membrane, cholesterol accounts for over 20% of plasma membrane lipids. Meanwhile, cholesterol is one of the important components of the liposome membranes. It has been found that cholesterol can maintain the fluidity of membrane.<sup>22</sup> As a component of the biofilm, cholesterol exist excellent biocompatibility.<sup>23</sup> Because of all these properties, cholesterol is important to membrane fusion, which is an essential procedure for endocytosis.<sup>24,25</sup> Then, it is expected that the anti-tumor drug modified with cholesterol will display enhanced ability of cellular uptake to increase their therapeutic effect and decrease the side effects.

In this study, cholesteryl hemisuccinate was used to modify gemcitabine to give CHSdFdC prodrug. The prodrug could self-assemble into nanoparticles in aqueous media. The properties of the nanoparticles were investigated, such as critical micelle concentration (CMC), mean particle size and size distribution, zeta potential, morphology and colloidal stability. The process of drug release from the nanoparticles and cellular uptake by Bxpc-3 cells *in vitro* were investigated in detail. Meanwhile, we assayed the ability of inhibiting the growth of Bxpc-3 cells of the prodrug *in vitro*. The nanoparticles have the capability to realize intracellularly controlled release of gemcitabine and reduce side effects because amide bond of the prodrug nanoparticles can be degraded by cathepsin B, an enzyme exists in lysosome.

## 2 Experimental

### 2.1 Materials and cells

Cholesterol was purchased from J & K Chemical Ltd. Gemcitabine hydrochloride was purchased from Shang Hai PuYi Chemical Co., Ltd. Gemcitabine base was purchased from Shanghai Demo Medical Tech Co., Ltd. EDCI and DMAP was purchased from Energy Chemical. Other chemicals were purchased from Sinopharm Chemical Reagent Co., Ltd. DCM, DMF and THF were dried and redistilled before use.

The Bxpc-3 cell line is a kind of human pancreatic cancer cell line, which was purchased from the Institute of Biochemistry & cell Biology, Chinese Academy of Science.

### 2.2 Characterization of compounds

<sup>1</sup>H NMR spectra were recorded with a Bruker Avarice TM 400 NMR spectrometer. The Fourier transform infrared spectra (FT-IR) were obtained with a Nicolet Nexus 670 spectrometer. The samples were pressed into pellets with KBr.



### 2.3 Synthesis of cholesteryl hemisuccinate-gemcitabine (CHSdFdC)

Succinic anhydride (1.2 mmol) was added to stirred solution of cholesterol (1.0 mmol) in toluene. The mixture was refluxed for 3 h, cooled to room temperature and filtered. The precipitate was collected and recrystallized with ethanol for twice, the cholesteryl hemisuccinate was obtained (yield: 82.8%). IR (neat,  $\text{cm}^{-1}$ ) 3442 (–OH), 2943–2860 (–CH<sub>2</sub>–), 1712 (–C=O), 1176 (C–O–C). <sup>1</sup>H NMR (400 MHz, CDCl<sub>3</sub>)  $\delta$ : 0.68 (3H, s, 20-H), 0.8–2.4 (28H, 1-H<sub>2</sub>, 3-H<sub>2</sub>, 6-H<sub>2</sub>, 8-H<sub>2</sub>, 9-H<sub>1</sub>, 10-H<sub>1</sub>, 11-H<sub>1</sub>, 13-H<sub>2</sub>, 14-H<sub>2</sub>, 15-H<sub>2</sub>, 16-H<sub>2</sub>, 17-H<sub>1</sub>, 21-H<sub>1</sub>, 22-H<sub>2</sub>, 24-H<sub>2</sub>, 25-H<sub>2</sub>, 26-H<sub>1</sub>), 0.87 (6H, d,  $J = 6.4$  Hz, 27-H<sub>3</sub>, 28-H<sub>3</sub>), 0.92 (3H, d,  $J = 6$  Hz, 23-H<sub>3</sub>), 1.02 (3H, s, 19-H<sub>3</sub>), 2.61 (2H, m, COCH<sub>2</sub>), 2.68 (2H, m, CH<sub>2</sub>CO), 4.64 (1H, m, 2-H<sub>1</sub>), 5.37 (1H, m, 7-H<sub>1</sub>).

Triethylamine (1.4 mmol) was added to stirred solution of cholesteryl hemisuccinate (1.2 mmol) in anhydrous THF (3 mL), under nitrogen. The mixture was cooled to –15 °C, and the solution of isobutyl chloroformate (1.2 mmol) in anhydrous THF (3 mL) was added dropwise. The mixture was stirred at –15 °C for 15 min and the solution of gemcitabine hydrochloride (1.2 mmol) and triethylamine (1.4 mmol) in anhydrous DMF (5 mL) was added dropwise to the mixture at the same temperature, then the mixture was stirred for another 0.5 h at –15 °C. After being stirred for 72 h at room temperature, the reaction mixture was concentrated. Aqueous sodium hydrogen carbonate was added and the mixture was extracted with DCM (3  $\times$  50 mL). The combined extracts were washed with water, dried over MgSO<sub>4</sub>, and concentrated. The crude product was purified by chromatography on silica gel eluting with 1–5% methanol in dichloromethane to give cholesteryl hemisuccinate-gemcitabine as amorphous white solid (yield: 32%). IR (neat,  $\text{cm}^{-1}$ ) 3500 (–CO–NH–), 3000 (–C=C–), 1665 (–CO–NH–), 1400 (–CO–NH–), 1065 (C–O). <sup>1</sup>H NMR (400 M, DMSO-d<sub>6</sub>)  $\delta$ : 0.65 (3H, s, 45-H<sub>3</sub>), 0.85 (6H, dd, 52-H<sub>3</sub>, 53-H<sub>3</sub>), 0.90 (3H, d, 48-H<sub>3</sub>), 0.96 (3H, s, 44-H<sub>3</sub>), 0.8–2.4 (28H, 28-H<sub>2</sub>, 31-H<sub>2</sub>, 32-H<sub>2</sub>, 34-H<sub>2</sub>, 35-H<sub>1</sub>, 36-H<sub>1</sub>, 37-H<sub>1</sub>, 39-H<sub>2</sub>, 40-H<sub>2</sub>, 41-H<sub>2</sub>, 42-H<sub>2</sub>, 43-H<sub>1</sub>, 46-H<sub>1</sub>, 47-H<sub>2</sub>, 49-H<sub>2</sub>, 50-H<sub>2</sub>, 51-H<sub>1</sub>), 2.56 (2H, m, COCH<sub>2</sub>), 2.69 (2H, m, CH<sub>2</sub>CO), 3.66 (1H, m, 6-H<sub>1</sub>), 3.80 (1H, d, 10-H<sub>1</sub>), 3.89 (1H, d, 10-H<sub>1</sub>), 4.19 (1H, m, 11-H<sub>1</sub>), 4.45 (1H, m, 27-H<sub>1</sub>), 5.28 (1H, t, 33-H<sub>1</sub>), 5.34 (1H, d, 8-H<sub>1</sub>), 6.18 (1H, t, 12-H<sub>1</sub>), 6.31 (1H, d, 9-H<sub>1</sub>), 7.24 (1H, d, 15-H<sub>1</sub>), 8.24 (1H, d, 14-H<sub>1</sub>), 11.08 (1H, s, 20-H<sub>1</sub>).

### 2.4 Nanoparticle fabrication and the critical micelle concentration

The CHSdFdC (5 mg) was dissolved in 10 mL THF, and the solution was added dropwise into 10 mL ultrapure MilliQ® water with constant stirring at 500 rpm. After stirring, the solution was loaded into a dialysis tube (MWCO 1000) and dialyzed against 12 L (4 L  $\times$  3) deionized water for 24 h.

The critical micelle concentration (CMC) was determined using pyrene as a fluorescence probe.<sup>26</sup> The concentration of CHSdFdC varied from  $2 \times 10^{-4}$  to  $0.1 \text{ mg mL}^{-1}$  with a fixed pyrene concentration of  $6 \times 10^{-7} \text{ mol L}^{-1}$ . The fluorescence spectra were measured on an F-4500 fluorescence spectrophotometer (Hitachi F-4500) with an excitation wavelength of 335 nm. The  $I_{373}/I_{384}$  ratio of the fluorescence intensity in the

emission spectra of pyrene was analyzed for the calculation of the CMC. The experiment was performed in triplet. The mean and corresponding standard deviations (mean  $\pm$  SD) are shown in the results.

### 2.5 Formulation and characterization of CHSdFdC nanoparticles

CHSdFdC nanoparticles were prepared by nanoprecipitation. Briefly, CHSdFdC (5 mg) was dissolved in THF (5 mL) and the solution was added dropwise into 10 mL ultrapure MilliQ® water under constant stirring at 500 rpm. The form of CHSdFdC nanoparticles occurred spontaneously. THF was completely evaporated using a rotary evaporator at 37 °C to obtain an aqueous suspension of pure CHSdFdC nanoparticles. The nanoparticles suspension has been analyzed using RP-HPLC to verify the actual concentration of CHSdFdC in the final product.

The mean particle size, size distribution, polydispersity index (PDI) and zeta potential were determined using dynamic light scattering (DLS) (ZetasizerNano ZS, Malvern Instruments, UK). The measurements were made after dilution of the nanoparticles suspension with ultrapure MilliQ® water.

The morphology of the nanoparticles was observed by transmission electron microscopy (TEM) (JM-2100, Japanese). A drop of aqueous nanoparticles suspension was deposited onto a 300 mesh copper grid coated with a thin carbon film. The grids were dried at room temperature and observed by TEM.

### 2.6 Colloidal stability of nanoparticles

The colloidal stability of nanoparticles was investigated by measuring variation of mean particle size of the nanoparticles. The nanoparticles were diluted with PBS to maintain the final concentration of CHSdFdC was  $2 \text{ mg mL}^{-1}$  and stored at 4 °C for 28 days. Meanwhile, the nanoparticles were diluted with cell culture medium (RPMI 1640 (Gibco BRL, Paris, France)) to maintain the final concentration of CHSdFdC was  $2 \text{ mg mL}^{-1}$  and incubated at 37 °C for 10 days. The experiment was performed in triplet. The mean and corresponding standard deviations (mean  $\pm$  SD) are shown in the results.

### 2.7 Cell line and culture

Human pancreatic cancer cell line Bxpc-3 was purchased from the Institute of Biochemistry & cell Biology, Chinese Academy of Science. Bxpc-3 cells were cultured in RPMI 1640 (Gibco BRL, Paris, France) supplemented with 10% fetal bovine serum (FBS, Hyclone, Logan UT) and 1% penicillin and streptomycin. The cell line was incubated at 37 °C in humidified 5% CO<sub>2</sub> atmosphere. When a cell confluence of 90% was reached, they were routinely trypsinized and subcultured.

### 2.8 Drug release from the CHSdFdC nanoparticles

Release of gemcitabine from the CHSdFdC nanoparticles in an aqueous buffer solution at different pH values (pH 5.0, pH 7.4) was measured by RP-HPLC with an Agilent 1200 (Agilent Technologies INC., Shanghai Branch) using a Zorbax Eclipse XDB-C18 column (5  $\mu\text{m}$ , 4.6 mm  $\times$  250 mm) at 30 °C. The



CHSdFdC (1 mg mL<sup>-1</sup> in DMSO), 60 µL, was dispersed in 2 mL of three different media including PBS (pH 7.4), sodium acetate buffer solution (pH 5.0), sodium acetate buffer solution (pH 5.0) contained 60 µL cathepsin B (U-activity unit = 10 U mL<sup>-1</sup>). The samples were kept in a THZ-C isothermal shaker at 37 °C and 150 rpm. At the predetermined time point, 100 µL of the sample solution was withdrawn, and same amount of acetonitrile was added immediately. The accumulative drug release was measured by RP-HPLC using methanol as the mobile phase. The flow rate of the mobile phase was 1 mL min<sup>-1</sup>. The Agilent 1200 Uv/vis detector was set at 254 nm. The release percentage of dFdC was calculated from the ratio of peaks area assigned to free dFdC and CHSdFdC. The experiment was performed in triplet. The mean and corresponding standard deviations (mean ± SD) are shown in the results. The cathepsin B is a kind of lysosomal enzyme which does not exist in human blood.<sup>27,28</sup> It is reported that the pH value of lysosome is about 5.0.<sup>29</sup> What we expect is that the prodrug is stable when it circulates in human blood whereas it can be degraded with presence of cathepsin B to release controlled release of dFdC from CHSdFdC prodrug. In the paper, the PBS with pH 7.4 was used to simulate the pH value of human blood, pH 5.0 buffer solution with cathepsin B was used to simulate the condition of lysosome, pH 5.0 buffer solution without cathepsin B was used to clarify that cathepsin B is an indispersable trigger in the controlled drug release.

## 2.9 *In vitro* ability of inhibiting the growth of Bxpc-3 cells assay

The ability of inhibiting the growth of tumor cells of CHSdFdC nanoparticles was investigated and compared with dFdC as positive control by MTT [3-(4,5-dimethylthiazol-2-yl)-2,5-diphenyl tetrazolium bromide] assay against Bxpc-3 cell line. Briefly, 4000 cells per well were incubated in 100 µL of complete culture medium (RPMI 1640 (Gibco BRL., Paris, France) supplemented with 10% fetal bovine serum (FBS, HvClone, Logan UT) and 1% penicillin and streptomycin) in 96-well plates for 24 h. The cells were then exposed to a series of concentrations of CHSdFdC nanoparticles, free dFdC or free CHS in 100 µL fresh complete culture medium for 72 h. The drug concentration in the case of CHSdFdC nanoparticles is equivalent to dFdC concentration. At the end of the incubation period, 20 µL of MTT solution (5 mg mL<sup>-1</sup>) in PBS was added to each well. The culture medium was gently replaced by 100 µL of dimethylsulfoxide in order to dissolve the formazan crystals after 4 h incubation. The optical density (OD) was measured at 570 nm with an automatic BIO-TEK microplate reader (Powerwave XS, USA), and the cell viability was calculated through the following equation:

$$\text{Cell viability (\%)} = (\text{OD}_{\text{sample}}/\text{OD}_{\text{control}}) \times 100\%. \quad (1)$$

The OD<sub>sample</sub> represents an OD value from a well that treated with samples, and OD<sub>control</sub> comes from a well that treated with cell culture medium only. Each experiment was performed in sextuplet. The mean and corresponding standard deviations (mean ± SD) are shown in the results.

## 2.10 Cellular uptake

The cellular uptake of CHSdFdC nanoparticles was quantitatively measured by RP-HPLC. The Bxpc-3 cells were seeded in 6-wells plate at a density of  $2.5 \times 10^5$  cells per well in 2 mL of culture medium and incubated for 24 h. The original cell culture medium was replaced with 2 mL fresh culture medium contained dFdC and CHSdFdC (dFdC: 0.1 mg mL<sup>-1</sup>). The cells were cultured for another 0.5 h, 1.5 h and 2.5 h, respectively. At the predetermined time point, the cell culture medium was discarded, and 2 mL of 1% SDS was added to make cell membrane lytic after the wells were washed with cold PBS for three times carefully. The cell lysate was dissolved in 200 µL mixture of methanol and acetonitrile (v/v = 1 : 1) after freeze drying. The concentrations of dFdC and CHSdFdC were measured by RP-HPLC. Experiments were carried in triplicates. Means and corresponding standard deviations (mean ± SD) were shown as results.

## 2.11 Statistical data analysis

Statistical data analysis was performed using Student's *t*-test.

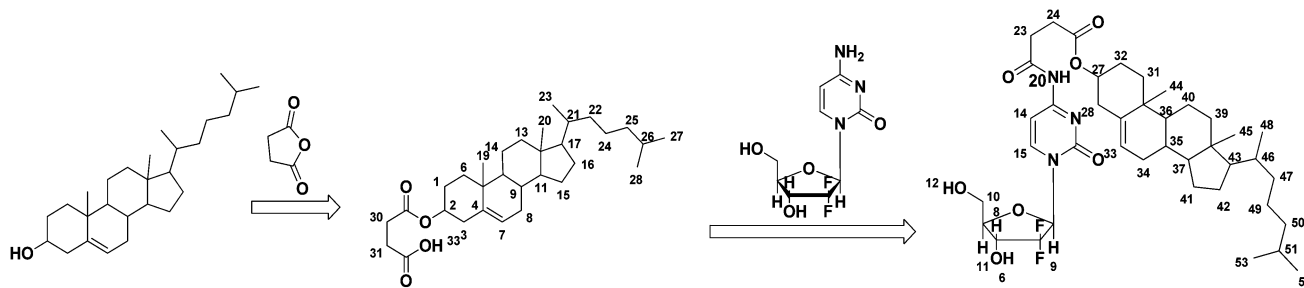
# 3 Results and discussion

## 3.1 Synthesis of cholesteryl hemisuccinate-gemcitabine (CHSdFdC)

Cholesteryl hemisuccinate was synthesized through esterification reaction between cholesterol and succinic anhydride. During the reaction, DMAP was used as catalysis. The synthesis scheme of cholesteryl hemisuccinate is shown in Scheme 1. The structure of the product was confirmed by NMR, and the detailed data of the chemical shifts are displayed in part 2.3. The structure was confirmed from the appearance of the peaks at 2.61 and 2.68 ppm which belong to succinic anhydride, 0.68, 0.87, 0.92, 1.02, 4.64, 5.37 ppm which belong to cholesterol. The ratio of succinic acid to cholesterol was equal to 1 : 1, which was confirmed by calculation of the integral ratios of the protons at 5.37 ppm (multiplet) assigned to 7-H signal of cholesterol and 2.61 ppm (multiplet) assigned to the methylene protons signal of succinic acid. In order to further confirm the structure of the product, Fourier transform infrared spectra were recorded. The FT-IR spectra data showed a new absorption appearance located at 1712 cm<sup>-1</sup> assigned to carboxyl group and 3442 cm<sup>-1</sup> assigned to hydroxyl group.

The CHSdFdC was synthesized through covalently coupling the amino group of gemcitabine on pyridine ring and the carboxyl group of cholesteryl hemisuccinate. The synthesis scheme is shown in Scheme 1. The structure was confirmed by NMR, and the detailed data of the shifts are displayed in part 2.3. The structure was confirmed from the appearance of the peaks at 11.08 ppm, which belong to amide bond and the disappearance of the peaks at 7.41 ppm which belong to the amino group of gemcitabine. The integral ratios of the protons at 11.08 ppm (single) assigned to amide proton signal and 0.65 ppm (single) assigned to the methyl protons signal of cholesteryl hemisuccinate were 1 : 3, indicating that the ratio of gemcitabine and cholesteryl hemisuccinate in the CHSdFdC





Scheme 1 Synthesis scheme of cholesteryl hemisuccinate–gemcitabine (CHSdFdC).

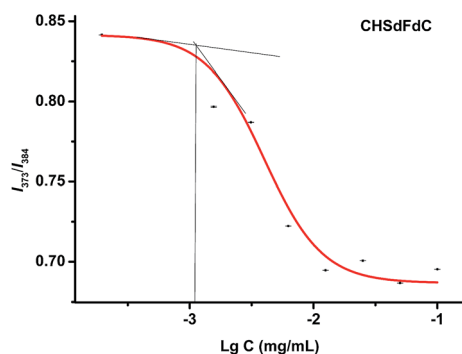


Fig. 2 Intensity ratios  $I_{373}/I_{384}$  of the pyrene emission fluorescence spectra as a function of the logarithm concentration of the CHSdFdC (means  $\pm$  SD,  $n = 3$ ).

was equal to 1 : 1. In order to further confirm the structure of CHSdFdC, Fourier transform infrared spectra were recorded. The FT-IR spectra data showed a new absorption appearance located at  $3500\text{ cm}^{-1}$  assigned to the amide bond.

### 3.2 CMC measurement of CHSdFdC

The CHSdFdC formed nanoparticles in aqueous media due to its amphiphilic structure. CMC was measured by fluorospectrophotometer with pyrene as a probe. The plot of the intensity ratio  $I_{373}/I_{384}$  of the pyrene emission spectra against the logarithm of the CHSdFdC concentration is shown in Fig. 2. The CMC value can be determined at the CHSdFdC concentration of onset of the  $I_{373}/I_{384}$  ratio decrease. When the concentration of CHSdFdC reaches the CMC, there is a sudden change of  $I_{373}/I_{384}$  in the fluorescence spectra due to the transfer of pyrene from a polar environment to a non-polar environment caused by the formation of nanoparticles. The CMC of CHSdFdC is  $0.001\text{ mg mL}^{-1}$ , as shown in Fig. 2. The CMC of CHSdFdC was very low, indicating it is rather stable against dilution.

### 3.3 Characterization of the nanoparticles

Particle size is an important factor that affects their *in vivo* performance and pharmacokinetics for nanoparticles. Tumors, unlike most healthy tissues, possess a leaky vasculature that allows the passage of colloidal particles with size in the range of 50–200 nm.<sup>30–32</sup> In this research, the mean particle size and size distribution, zeta potential were measured by DLS in aqueous

media at room temperature. The mean particle size was 200 nm, as shown in Fig. 3A. The main hydrodynamic diameter of the CHSdFdC nanoparticles was between 40 and 500 nm. This demonstrated that the nanoparticles were able to pass through the large pores of the tumor blood vessel to target the tumor tissue. The nanoparticles showed negative potential at around  $-0.06\text{ mV}$  in the measurement of zeta potential, suggesting potential capacity for prolonging the circulation time in blood because nanoparticles with positive surface charges are inclined to agglomerate due to interaction with serum protein in human blood.<sup>33</sup>

The morphology of the nanoparticles was observed by transmission electron microscopy (TEM), as shown in Fig. 3B and C. The mean particle size was approximately 200 nm in a dehydrated state. The size measured by TEM was very close to that measured by DLS in aqueous media.

### 3.4 Colloidal stability of CHSdFdC nanoparticles

The colloidal stability of the nanoparticles was investigated by measuring the variation of mean particle size. The nanoparticles were diluted with PBS and stored at  $4\text{ }^{\circ}\text{C}$  for 28 days. This is the storage condition for CHSdFdC nanoparticles

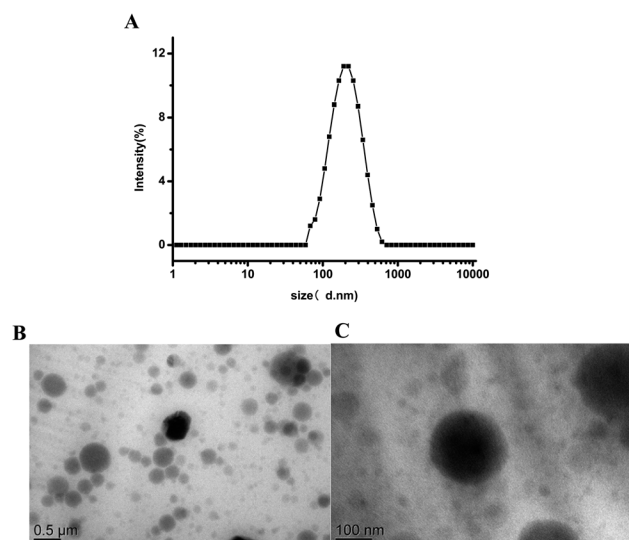


Fig. 3 (A) Size and size distribution of CHSdFdC nanoparticles (B and C) transmission electron microscopy (TEM) of CHSdFdC nanoparticles.



suspension. Meanwhile, the nanoparticles were diluted with cell culture medium (RPMI 1640 (Gibco BRL, Paris, France)) and incubated at 37 °C for 10 days. This condition was used to simulate the human plasma, in order to assay the stability of CHSdFdC nanoparticles when it circulates in human plasma. It demonstrated that the CHSdFdC nanoparticles are stable at 4 °C in PBS as well as at 37 °C in cell culture medium (RPMI 1640 (Gibco BRL, Paris, France)), with no significant variation of the mean particle size was observed, as shown in Fig. 4A and B.

### 3.5 Drug release from the CHSdFdC nanoparticles

The amide bond could be degraded by cathepsin B which exists in lysosome. Thus, there is possibility for dFdC to release from the CHSdFdC nanoparticles at the presence of cathepsin B. As shown in Fig. 5, the release of dFdC was very slow under weakly acid condition (pH 5.0 HOAc–NaOAc buffer solution) or neutral pH condition (pH 7.4 PBS), the amounts were 0.64% and 1.84% within 10 h, respectively. On the other hand, the release of dFdC was much faster under the weakly acid condition (pH 5.0 HOAc–NaOAc buffer solution) in the presence of cathepsin B, the accumulative amount of drug release reached up to 80% within 10 h. These results demonstrated the CHSdFdC nanoparticles had great potential to realize intracellular release of dFdC.

### 3.6 *In vitro* ability of inhibiting growth of Bxpc-3 cells assay

The *in vitro* ability of inhibiting growth of tumor cells of the CHSdFdC nanoparticles was evaluated with a human pancreatic cancer cell line Bxpc-3 *via* MTT assay. Representative concentration–growth inhibition curves showed the effects of treatment with free dFdC and CHSdFdC nanoparticles on the growth of Bxpc-3 cells after 72 h. As shown in Fig. 6, both free dFdC and CHSdFdC nanoparticles inhibited cell growth in a dose-dependent manner, whereas the latter was more toxic than the former at the same concentration. It was thought that the increased cytotoxicity of the CHSdFdC resulted from two reasons. On one hand, CHSdFdC nanoparticles possess enhanced ability of cellular uptake, which make it easier to enter tumor cells. This was confirmed by the cellular uptake experiment. On the other hand, the released CHS, due to the degradation of CHSdFdC nanoparticles prodrug by cathepsin B, also demonstrated ability of inhibiting the growth of Bxpc-3

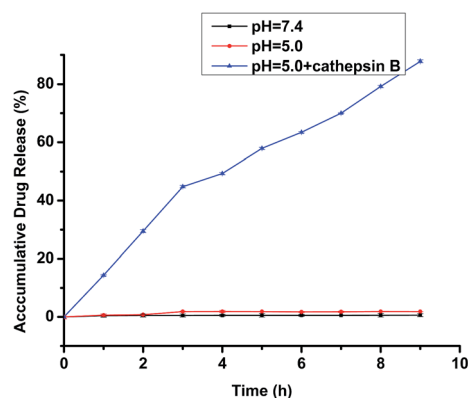


Fig. 5 Accumulative drug release of dFdC from CHSdFdC nanoparticles at 37 °C.

cells, especially at high concentration as shown in Fig. 6. It has been reported that CHS could incorporate into cell membrane to inhibit cell proliferation.<sup>34</sup> Only when the concentration of CHS reaches a certain high level, the cytotoxicity could be observed. And the result in this paper is consistent with the reported result.<sup>34</sup>

### 3.7 Cellular uptake

In order to confirm the hypothesis that the ability of cellular uptake of CHSdFdC nanoparticles is enhanced than dFdC, the amount of cellular uptake of CHSdFdC nanoparticles was measured by RP-HPLC, in the measurement, dFdC was used as control. As shown in Fig. 7, the cellular uptake amount of CHSdFdC nanoparticles varied apparently while that of dFdC varied little, which is 15 folds of dFdC at the same culture period of 2.5 h. The conclusion was drawn that CHSdFdC nanoparticles could penetrate the cells much more easily than free dFdC, which improved the efficacy of inhibiting growth of tumor cells. The result in this paper showed that the CHSdFdC nanoparticles could be internalized much more easily than free dFdC, this result is related to the different uptake mechanism of dFdC and CHSdFdC nanoparticles. But the cytotoxic activity of the drug and the prodrug are similar, this result is due to the

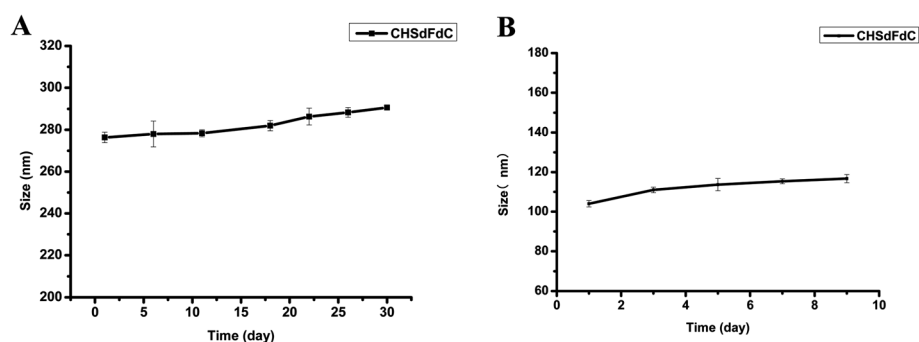


Fig. 4 (A) Variation of the mean particle size of CHSdFdC nanoparticles at 4 °C in PBS (B) variation of the mean particle size of CHSdFdC nanoparticles at 37 °C in cell culture medium (means  $\pm$  SD,  $n = 3$ ).



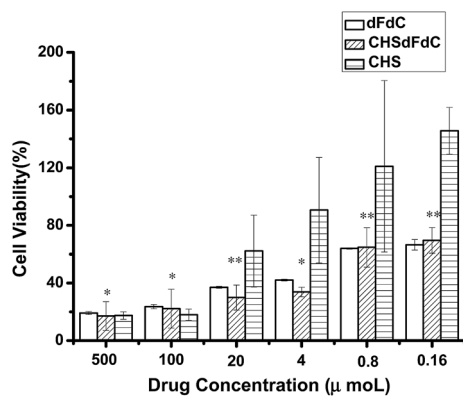


Fig. 6 Cellular uptake of dFdC and CHSdFdC.

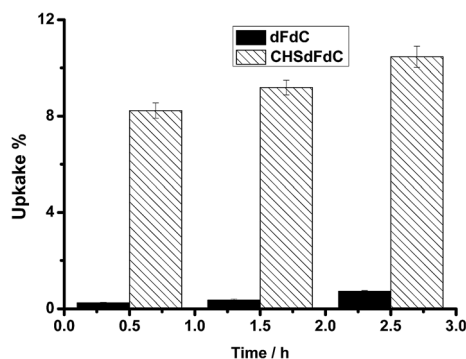


Fig. 7 Cell viability of free dFdC, CHSdFdC nanoparticle and CHS.

incomplete cleavage of CHSdFdC to release dFdC which actually demonstrate the effect of inhibiting cells growth.

## 4 Conclusions

The amphiphilic prodrug, CHSdFdC, which can self-assemble in aqueous media spontaneously to form nanoparticles, was synthesized. The mean particle size of the nanoparticles is about 200 nm and the zeta potential is  $-0.06$  mV. The nanoparticles are relatively stable at storage condition and simulated human plasma. Compared with free gemcitabine, the nanoparticles exhibited increased ability of cellular uptake and inhibiting the growth of Bxpc-3 cells *in vitro*. Moreover, the CHSdFdC nanoparticles prodrug displayed intracellularly controlled drug release of gemcitabine from the nanoparticles. The nanoparticles provide a new approach to deliver gemcitabine to cancer cells. Generally speaking, the CHSdFdC has a great potential as prodrug for pancreatic cancer and other tumor therapy.

## Acknowledgements

The research work was supported by the International Science & Technology Cooperation Program of China, Ministry of Science and Technology of China (2013DFG32340), Shanghai Municipality Commission for Special Project of Nanometer Science

and Technology (11nm0506000), the National Natural Science Foundation of China (81171333) and the EU-FP 7 project (MARINA 263215).

## References

- 1 B. Lund, O. P. Hansen, K. Theilade, M. Hansen and J. P. Neijt, *J. Natl. Cancer Inst.*, 1994, **86**, 1530–1533.
- 2 H. Anderson, B. Lund, F. bach, N. Thatcher, J. Walling and H. H. Hansen, *J. Clin. Oncol.*, 1994, **12**, 1821–1826.
- 3 G. Catimel, J. B. Vermorken and M. Clavel, *et al.*, *Ann. Oncol.*, 1994, **5**, 543–547.
- 4 J. R. Mackey, R. S. Mani, M. Selner, D. Mowles, J. D. Young, J. S. Bett, C. R. Crawford and C. E. Cass, *Cancer Res.*, 1998, **58**, 4349–4357.
- 5 D. Peer, J. M. Karp, S. Hong, O. C. Farokhzad, R. Margalit and R. Langer, *Nat. Nanotechnol.*, 2007, **2**, 751–760.
- 6 F. M. Kievit and M. Zhang, *Adv. Mater.*, 2011, **23**, 217–247.
- 7 M. Ding, J. Li, X. He, N. Song, H. Tan, Y. Zhang, L. Zhou, Q. Gu, H. Deng and Q. Fu, *Adv. Mater.*, 2012, **24**, 3639–3645.
- 8 M. T. Basel, T. B. Shrestha, D. L. Troyer and S. H. Bossmann, *ACS Nano*, 2011, **5**, 2162–2175.
- 9 T. M. Allen and P. R. Cullis, *Science*, 2004, **303**, 1818–1822.
- 10 M. Ferrari, *Nat. Rev. Cancer*, 2005, **5**, 161–171.
- 11 M. E. Davis, Z. Chen and D. M. Shin, *Nat. Rev. Drug Discovery*, 2008, **7**, 771–782.
- 12 E. K. Chow, X. Q. Zhang, M. Chen, R. Lam, E. Robinson, H. Huang, D. Schaffer, E. Osawa, A. Goga and D. Ho, *Sci. Transl. Med.*, 2011, **3**, 73–93.
- 13 J. A. Barreto, W. O. Malley, M. Kubeil, B. Graham, H. Stephan and L. Spiccia, *Adv. Mater.*, 2011, **23**, 18–40.
- 14 A. Schroeder, D. A. Hever, M. M. Winslow, J. E. Dahlman, G. W. Pratt, R. Langer, T. Jacks and D. G. Anderson, *Nat. Rev. Cancer*, 2012, **12**, 39–50.
- 15 R. K. Jain and T. Stylianopoulos, *Nat. Rev. Clin. Oncol.*, 2010, **7**, 653–664.
- 16 W. J. Gradishar, S. Tjulandin, N. Davidson, H. Shaw, N. Desai, P. Bhar, M. Hawkins and J. O'Shaughnessy, *J. Clin. Oncol.*, 2005, **23**, 7794–7803.
- 17 T. Neff and C. A. Blau, *Exp. Hematol.*, 1996, **24**, 1340–1346.
- 18 L. H. Reddy, C. Dubernet, S. L. Mouelhi, P. E. Marque, D. Desmaele and P. Couvreur, *J. Controlled Release*, 2007, **124**, 20–27.
- 19 S. Rejiba, L. H. Reddy, C. Bigand, C. Parmentier, P. Couvreur and A. Hajri, *Nanomedicine*, 2011, **7**, 841–849.
- 20 V. Allain, C. Bourgaux and P. Couvreur, *Nucleic Acids Res.*, 2012, **40**, 1891–1903.
- 21 W.-G. Chung, M. A. Sandoval, B. R. Sloat, D. S. P. Lansakara P and Z. Cui, *J. Controlled Release*, 2012, **157**, 132–140.
- 22 I. Tabas, *J. Clin. Invest.*, 2002, **110**, 905–911.
- 23 X. Tan, *et al.*, *Anal. Biochem.*, 2005, **337**, 111–120.
- 24 Z. Chen and R. P. Rand, *Biophys J.*, 1997, **73**, 267–276.
- 25 M. C. Kielian and A. Helenius, *J. Virol.*, 1984, **52**, 281–283.
- 26 R. Duncan, L. W. Seymour and K. B. O'Hare, *et al.*, *J. Controlled Release*, 1992, **19**, 331–346.
- 27 J. S. Mort and D. J. Buttle, *Int. J. Biochem. Cell Biol.*, 1997, **29**, 715–720.



- 28 O. Vasiljeva and B. Turk, *Biochimie*, 2008, **90**, 380–386.
- 29 S. Ohkuma and B. Poole, *Proc. Natl. Acad. Sci. U. S. A.*, 1978, **75**, 3327–3331.
- 30 F. Yuan, M. Leunig, S. K. Huang and D. A. Berk, *Cancer Res.*, 1994, **54**, 3352–3356.
- 31 R. K. Jain, *Adv. Drug Delivery Rev.*, 1997, **26**, 71–90.
- 32 N. Z. Wu, D. Da, T. L. Rudoll and D. Needham, *et al.*, *Cancer Res.*, 1993, **53**, 3765–3770.
- 33 X. Zhang, F. Du and J. Huang, *Colloids Surf., B*, 2012, **100**, 155–162.
- 34 Z. Djuric, L. K. Heilbrun, S. Lababidi, C. K. Everett-Bauer and M. W. Fariss, *Cancer Lett.*, 1997, **111**, 133–139.